INTERNATIONAL SCIENTIFIC JOURNAL
GEOGRAPHICA PANNONICA
Volume 28, Issue 1, 1–20 (March 2024)
Contents lists available at ScienceDirect
Journal homepage: http://www.dgt.uns.ac.rs/en/homepage/pannonica/

Monitoring and Predicting Land Use/Land Cover Dynamics in Djelfa City, Algeria, using Google Earth Engine and a Multi Layer Perceptron Markov Chain Model

Hamza Bendechou[A*], Ahmed Akakba[A], Mohammed Issam Kalla[A], Abderrahmane Ben Salem Hachi[B]

[A] *Laboratory of natural hazards and spatial planning (LRNAT), Earth and Universe Sciences Institute, University of Batna 2, Batna, Algeria; h.bendechou@univ-batna2.dz, a.akakba@univ-batna2.dz, m.kalla@univ-batna2.dz*

[B] *Department of Earth and Universe Sciences, University Ziane Achour of Djelfa, Djelfa, Algeria; iha2007hachi@gmail.com*

KEYWORDS

Land use/land cover
Google Earth Engine
Support vector machine
Multi Layer Perceptron
Markov Chain
Djelfa city

ABSTRACT

Understanding the historical and projected changes in land use and land cover (LULC) in Djelfa city is crucial for sustainable land management, considering both natural and human influences. This study employs Landsat images from the Google Earth Engine and the support vector machine (SVM) technique for LULC classification in 1990, 2005, and 2020, achieving over 90% accuracy and kappa coefficients above 88%. The Land Change Modeler (LCM) was used for detecting changes and predicting future LULC patterns, with Markov Chain (MC) and Multi Layer Perceptron (MLP) techniques applied for 2035 projections, showing an average accuracy of 83.96%. Key findings indicate a substantial urban expansion in Djelfa city, from 924.09 hectares in 1990 to 2742.30 hectares in 2020, with a projected increase leading to 1.6% of nonurban areas transitioning to urban by 2035. There has been significant growth in steppe areas, while forested, agricultural, and barren lands have seen annual declines. Projections suggest continued degradation of bare land and a slight reduction in steppe areas by 2035. These insights underscore the need for reinforced policies and measures to enhance land management practices within the region to cater to its evolving landscape and promote sustainable development.

Introduction

Land Use/Land Cover Change (LULCC) resulting from human activities is a well-recognized global phenomenon that has significantly transformed the Earth's terrestrial surface. Over the period from 1960 to 2019, approximately one-third of the Earth's land area underwent alterations (Winkler et al., 2021). While human-induced changes to land have been practised for thousands of years, the scale and pace of LULCC in recent times have escalated significantly, exerting profound effects at local, regional, and global scales. These changes are crucial for understanding the altered landscape, ecological stewardship, and future-oriented environmental planning (Dwivedi et al., 2005; Fan et al., 2007a; Zhao et al., 2004). In the last three centuries, global LULCC has been characterized by the expansion of agriculture at the expense of forested areas (Kolb et al., 2013; Pérez-Vega et al., 2012). This trend is particularly evident in Africa, where natural vegetation has given way to anthropogenic land uses (Barnieh et al., 2020;

* Corresponding author: Hamza Bendechou; email: bendechou@gmail.com

doi: 10.5937/gp28-47299

Received: October 23, 2023 | Revised: January 08, 2024 | Accepted: February 06, 2024

Bullock et al., 2021; Findell et al., 2017). Between 2012 and 2017, Africa experienced a substantial reduction in natural vegetation and an increase in impervious areas, primarily due to population growth and soil desiccation driven by climate change (Nowak & Greenfield, 2020). Various factors, including population growth, economic expansion, and physical variables like topography, climate, and soil composition, significantly influence land use and land cover changes (Skole & Tucker, 1993).

Choosing appropriate prediction and validation time intervals significantly influences the accuracy of predictions (Chen & Pontius, 2010). The accuracy of predictions can be influenced by the pace and nature of transitions within the selected time intervals. Utilizing a broader temporal scale for modeling land cover change might lead to an inadequate understanding of landscape change patterns, potentially compromising the overall performance of the model (Alvarez Martinez et al., 2011). Many research studies focusing on future land cover change tend to adopt relatively short to intermediate historical time scales, typically spanning 5 to 15 years.

Land use change is intricately linked to historical processes, reflecting how communities interact with and utilize their landscapes. In contemporary times, land use has evolved beyond habitation to encompass industrial ventures and tourism (Mather, 1986). Analyzing LULC changes is crucial for understanding global transformations across spatial and temporal dimensions (Lambin, 1997) and provides insights into human activities within specific environments (López et al., 2001).

However, the rapid global population growth has placed substantial pressure on land resources, leading to complex interactions among environmental factors (Green et al., 1994). Land use change is a dynamic process with nonlinear patterns that can initiate intricate feedback loops, affecting living conditions and community vulnerability. Therefore, evaluating land use change trajectories and projecting future scenarios is essential for establishing sustainable conditions.

Remote sensing technology offers a rapid and effective means of monitoring LULC changes due to its broad spatial coverage, frequent updates, and abundant data availability (Homer et al., 2020; Zhao et al., 2016). However, processing remote sensing data traditionally can be time-consuming and resource-intensive, especially for large-scale LULC information extraction. The emergence of cloud storage and computing technology, such as Google Earth Engine (GEE), has revolutionized the handling of extensive remote sensing data, making it a pivotal tool for monitoring land use changes (Gorelick et al., 2017). Satellite imagery, in particular, facilitates comprehensive monitoring of deforestation and landscape dynamics on a global scale (Noma et al., 2013; Oliveira, 2017).

The adoption of cloud-based platforms like GEE is essential for handling large-scale data efficiently, enabling the analysis of expansive spatial regions without the need for extensive data downloads (Fadli et al., 2019).

Many scholars have conducted research using GEE to monitor LULC changes, water resources, eco-environmental quality, and agricultural resources (Dong et al., 2016; Ermida et al., 2020; Hu et al., 2018; Li et al., 2021; MAO & LI, 2021; Wang et al., 2020; Xiong et al., 2017; Xiong et al., 2021).

Land Change Models, such as the Markov Chain Model (MC), Artificial Neural Networks (ANN), and the Land Change Modeler (LCM), play a significant role in environmental and geomatics research related to LULCC (Camacho Olmedo et al., 2015). Monitoring and analyzing LULC changes are essential for understanding current land use patterns and their alterations, facilitating sustainable development initiatives (Fan et al., 2007b). These models enhance our understanding of land use modifications driven by human activities (Brown et al., 2004).

Several methods, including the Markov chain (MC), artificial neural network (ANN), cellular automata (CA), CA-Markov, binary logistic regression (BLR), and similarity-weighted instance-based machine learning algorithms (MLA), are commonly employed to predict and simulate future LULC changes (Anand et al., 2018; Azari et al., 2016; Islam et al., 2018; Liu et al., 2017; Mozumder et al., 2016; Sinha et al., 2015). LCM stands out for its significance in capturing land cover changes and its applicability in various contexts (Halmy et al., 2015). However, no single model is superior to others, and the choice depends on specific research objectives (Alqadhi et al., 2021).

The integration of Multi Layer Perceptron (MLP) algorithms into LCM frameworks allows researchers to harness the power of MLP's ability to learn from historical data and generate projections for future land cover scenarios. MLP neural networks, with their input, hidden, and output layers, excel at capturing complex, nonlinear relationships (Siroosi et al., 2020). They are particularly useful when prior knowledge is limited, accommodating missing data and operating without stringent requirements, unlike some other models (Pontius et al., 2008).

Incorporating both natural and human factors into LULC dynamics is essential for projecting potential future scenarios. These driving forces can manifest as direct or indirect influences, making their consideration crucial for optimizing land use and sustainable planning (Behera et al., 2012).

The MLPNN algorithm was employed to map the significant potential transitions between different LULC classes (Larbi et al., 2019). As per Eastman (2020), MLP neural networks have been identified as the most robust approach for mapping transition potentials. While the logistic regression method remains a viable option, MLP neural networks offer the advantage of simultaneously modeling

multiple or even all transitions, making them highly adept at capturing nonlinear relationships (Eastman, 2020).

This study focuses on Djelfa city, Algeria, which has experienced significant growth and land use changes since its establishment in 1962. However, a comprehensive evaluation of these changes using remote sensing and GIS technology is lacking. Such an assessment is crucial for effective urban planning to address the challenges posed by rapid urbanization. The study aims to analyze land use transformations in Djelfa city, document temporal shifts, identify driving factors, and examine initiatives for managing these changes. Ultimately, the research seeks to provide valuable insights for sustainable urban planning and land management in Djelfa city.

Historical satellite images are used to monitor and analyze LULC changes, with a focus on predicting future changes under a business-as-usual scenario. Understanding past, current, and projected LULC changes is vital for effective land management in Djelfa city, considering ongoing socioeconomic transformations. The study utilizes GEE for SVM supervised classification, a high-performance machine learning algorithm renowned for its accuracy in LULC classification.

While existing research in Djelfa city using remote sensing images on the GEE platform is limited, this study fills the gap by providing a comprehensive 45-year assessment of land use changes, thus contributing valuable empirical data for land use policies and sustainable planning in the region. The research is instrumental in understanding the spatial dynamics of land use changes, preventing resource misallocation, and enhancing land management in Algeria.

Materials and methods

Study area

The study is focused on the capital city of Djelfa Province, situated in the central region of northern Algeria. It is positioned approximately 300 km south of the country's capital. The city is located within the geographic coordinates of 34° 31' to 34° 48' North latitude and 3° 4' to 3° 21' East longitude. Encompassing an area of 542.17 km², the study area exhibits distinct climatic features, predominantly classified as semi-arid. The prevailing climatic conditions in the study area are indicative of a semi-arid climate, characterized by an annual average precipitation ranging between 200 mm and 500 mm. The climate is typified by hot semi-arid summers, with maximum temperatures reaching up to 33 °C, contrasted by cold subtropical winters, during which temperatures can drop below 0°C. Geographically, the study area is situated within a region marked by plateaus, varying in altitude between 900 m and 1400 m (D.P.S.B, 2020) (Figure 1).

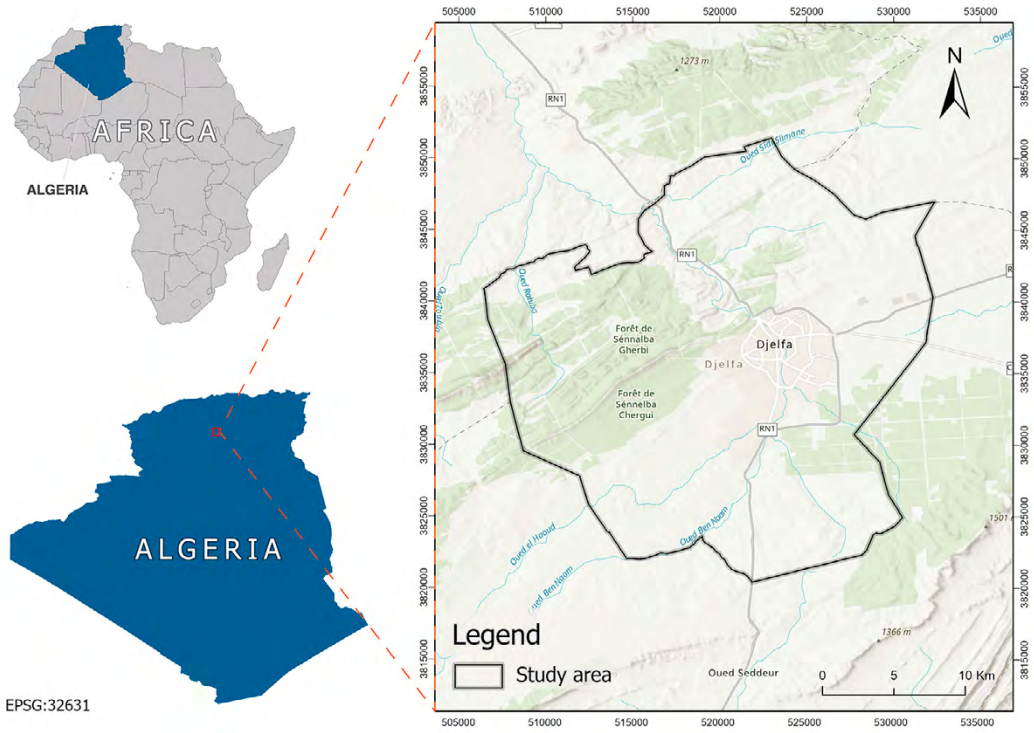

Figure 1. The study area
Source: ESRI Map including World Topographic Map and World Hillshade

Data collection

This study utilized data primarily from Landsat TM/OLI for remote sensing imagery, digital elevation model (DEM) for topographic analysis, and various geographic and socioeconomic datasets (Table 1). Specifically, we employed Landsat 5 TM for 1990 and 2005, and Landsat 8 OLI for 2020 due to their relevance in LULC analysis, detailed in Table 2. These images facilitate the identification of land use and land cover transitions (Midekisa et al., 2017) and were utilized as inputs for the analysis of land use and land cover changes. To clarify, classification was conducted on three individual years within the specified period (Feng et al., 2020; Rawat & Kumar, 2015), avoiding any implication of continuous annual study.

The term 'ground truth data' refers to actual observations used as training samples to develop the land classification model, detailed in Table 3. This includes data from field surveys and digitized high-resolution images from Google Earth. The employment of these ground truth data was critical in developing three distinct classified images for the respective years, reflecting the diverse LULC classes within Djelfa city (Wagle et al., 2020; Zadbagher et al., 2018).

Image preprocessing

In this study, GEE was utilized for its extensive repository of satellite imagery, known for radiometric and geometric corrections. Our preprocessing involved specific scaling

Table 1. Factors influencing the LULC changes.

Type	Code	Name	Source
Socioeconomic factors	TMI	Topographic map index	https://www.earthdata.nasa.gov/sensors/srtm Shuttle Radar Topography Mission (SRTM)
	DFR	Distance from roads	https://www.openstreetmap.org/ Downloaded the shapefile of Road Open Street distance method Map Road network (Town plan for the wilaya of Djelfa 2023)
	DFB	Distance from the built up land	https://earthexplorer.usgs.gov/ Downloaded the shapefile of built up area (Town plan for the wilaya of Djelfa 2023)
Natural factors	DFS	Distance to stream	https://www.hydrosheds.org/ Download toposheet map of study area
	SLP	Slope gradients	https://www.earthdata.nasa.gov/sensors/srtm Shuttle Radar Topography Mission (SRTM)
	ELV	Elevation	https://www.earthdata.nasa.gov/sensors/srtm Shuttle Radar Topography Mission (SRTM)

Table 2. Landsat image collections used for classification

Year	Satellite	Sensor	RBG composite bands	Spatial resolution	Period of collection
1990	Landsat	5-TM	3-4-5	30m	01/01/90–31/12/90
2005	Landsat	5-TM	3-4-5	30m	01/01/05–31/12/05
2020	Landsat	8-OLI	4-5-6	30m	01/01/20–31/12/20
TM Thematic Mapper, OLI Operational Land Image					

Source: USGS

Table 3. Number of Training samples of LULC units for 1990, 2005, and 2020

LULC units	Number of Training samples		
	1990	2005	2020
Urban Area	28	30	29
Agricultural Land	23	31	31
Forest Land	46	46	44
Steppe	29	29	29
Bare land	44	44	43
Total	170	180	176

techniques to adjust image values for true surface reflectance, crucial for accurate land cover classification (Carneiro et al., 2021; Mugiraneza et al., 2020; Roy et al., 2020). Cloud masking was conducted using a Landsat Simple Cloud Score algorithm, as influenced by the approaches outlined in (Carneiro et al., 2021). To further enhance the classification process, NDVI and NDBI indices were computed, serving as supplementary attributes to enrich the dataset with vital details on vegetation and built-up areas (Barnieh et al., 2020; Feng et al., 2016; Hackman et al., 2017, 2020; Prasomsup et al., 2020; Yu et al., 2014).

Topographic Analysis

In our methodology, the Topographic Index (TI) was calculated using the widely accepted formula developed by (Beven et al., 1984), utilizing Aster GDEM data. TI, which quantifies relative humidity, is integral to understanding moisture dynamics and their implications on land characteristics.

Analysis of Spatial Variables

The analysis of spatial variables was conducted using Cramer's V to distinguish between static and dynamic properties. Specifically, distance from roads and distance from settlements were identified as dynamic factors, while other variables were considered static. The derived Cramer's V values were adopted as weighting factors for the spatial variables and incorporated into the MC model for future projections. The transformation of categorical maps into continuous maps was facilitated using the Evidence Likelihood transformation, aiding in a more refined and comprehensive analysis of land cover transitions (Mas et al., 2014).

Image classification and accuracy assessment

In this study, we employed the GEE, an open-access cloud-based platform, for image collection, supervised classification, and accuracy assessment, utilizing AI machine learning algorithms. Specifically, the SVM classifier was used within the GEE for accurate LULC classification (Mantero et al., 2004; Wahap & Shafri, 2020). The GEE code editor was a valuable tool for analysis and customization via programming code. Training samples were crucial for this process and are detailed in Table 3. For each year, 70% of the samples were used for training the SVM classification algorithm, and the remaining 30% for testing, focusing on SVM's capability to minimize misclassified pixels (Shaharum et al., 2020). Quantitative accuracy of the classified LULC maps was measured using two key metrics: Overall Accuracy (OA) and the Kappa index (K). OA is the ratio of correctly classified pixels to the total number of pixels, and it's calculated using equation (1). The Kappa index measures agreement by chance in the classification process, and it's represented by equation (2).

$$OA = \left(\frac{\sum_{i=1}^{n} x_i}{N} \right) \cdot 100 \quad (1)$$

Where x_i represents the number of correctly classified pixels for each class and N is the total number of pixels.

$$K = \frac{\sum a - \sum ef}{N - \sum ef} \quad (2)$$

Where a is the frequency of correct classifications for each category, ef is the expected frequency of correct classifications by chance, and N is the total number of pixels.

We also implemented the MLP model to refine the land cover classification process, training it with 75% of the data and testing with the remaining 25%. This ensured robust predictive performance, with the optimal MLP training parameters detailed in Table 8. Support vectors in the SVM framework were instrumental in defining the hyperplane, thereby maximizing the separation between classes (Liu et al., 2020). This process and the resulting classified images are visualized in Figure 2.

Change detection and transition analysis using LCM

We utilized the LCM integrated with IDRISI Selva software to analyze and predict land use changes in Djelfa city for the periods 1990-2005 and 2005-2020, employing categorized maps from Landsat imagery (Abijith & Saravanan, 2022; Mishra et al., 2018; Shawul & Chakma, 2019). The LCM's application included:

- Calculating annual rate of change for each LULC class.
- Generating FROMTO change maps and spatial trend maps using a third-degree polynomial function (Eastman, 2020).
- Determining the extent of land surface change between LULC states to understand the dynamics over the designated periods (Singh, 1989).

In-depth evaluations of land use dynamics and biodiversity impacts were conducted, with the findings offering insights into the anthropogenic influences on various LULC classes. The percentage change is computed using Equation (3) to quantify the extent of changes (Hussien et al., 2023).

$$p = \frac{(AI - Ae) \cdot 100}{Ae} \quad (3)$$

Where AI is the area in a later LULC map, and Ae is the area in an earlier LULC map. The analysis utilized the post-classification approach for a comprehensive evaluation of LULC dynamics. The specific methodologies and

outcomes of LCM within the context of Djelfa city are now detailed and precise, addressing the need for specificity.

Consolidated Modeling and Prediction Analysis

For our LULC change prediction, the MLP and MC models were utilized (Mishra & Rai, 2016). The MLP model, noted for its 83.96% accuracy rate, facilitated the creation of potential change maps as crucial inputs for further MC analysis, aiming to project future land cover changes with associated probabilities (Gashaw et al., 2018). Initial modeling involved using transition potential images from key historical years as part of the predictive groundwork.

The study also integrated various natural and anthropogenic factors affecting land cover, utilizing a combination of topographic, demographic, and environmental data (Kim & Newman, 2020; Mirici et al., 2018). This integration was critical in predicting transition potentials and understanding the implications of various land cover drivers on future land use scenarios. An empirical analysis of shifts in land cover was conducted, focusing on quantifying changes and predicting future scenarios (Eastman, 2015; Karul & Soyupak, 2003). A rigorous validation phase followed the initial modeling to ensure the model's predictive accuracy (Chaudhuri & Clarke, 2014).

The simulation results from these models aimed to provide a nuanced understanding of the LULC changes over time. This involved mapping the gains and losses within distinct LULC classes to offer insights into the dynamics of land use changes and the effectiveness of our modeling approach (Hasan et al., 2020; Shaharum et al., 2020).

Model validation

The reliability of our predictive models was ensured through a rigorous validation process subsequent to the initial calibration phase. This involved a two-step approach where model parameters were first fine-tuned, followed by a rigorous assessment of predictive accuracy. The validation phase primarily utilized the Kappa coefficient, a widely recognized metric for measuring the accuracy of predictive models (Congalton, 1991; Singh et al., 2018). The process involved comparing forecasted LULC data gener-

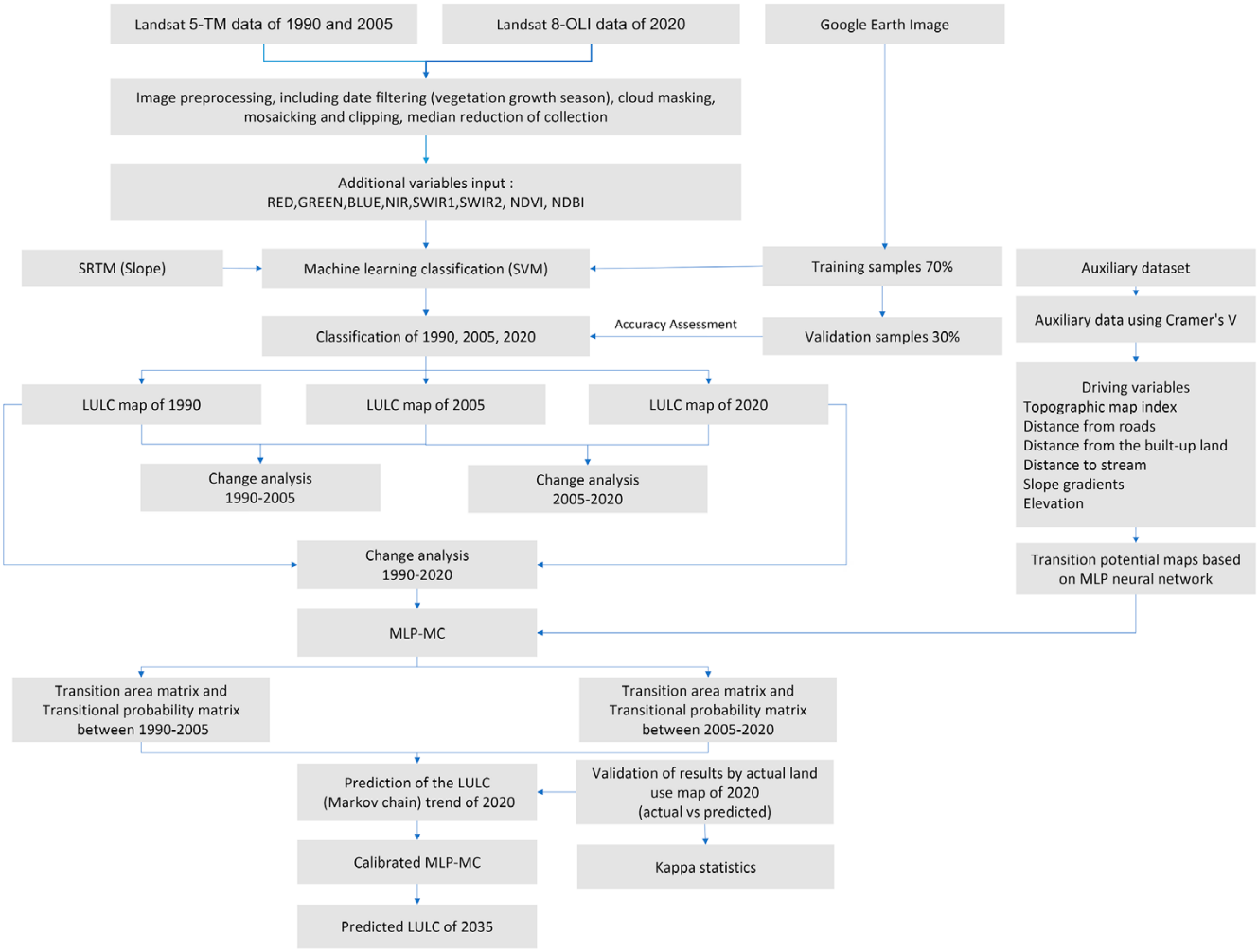

Figure 2. Overview of the methodology of LULC maps classification and prediction in the Djelfa city

ated by the model against a set of reference data to evaluate the model's predictions (Bununu, 2017; Congalton, 1991). Insights gained from this validation phase contributed to understanding the potential to project LULC scenarios for future years, thereby extending the applicability and relevance of the study's findings.

Results

Our key findings and conclusions can be summarized as follows:

LULC Mapping and Accuracy

The study conducted multitemporal LULC mapping for 1990, 2005, and 2020 with overall accuracies of 90%, 94%, and 94% respectively. Kappa coefficients indicated high reliability across all years. The SVM classification, visualized in Figure 3, and the detailed proportions in Table 4, revealed significant land cover dynamics over the three decades. A notable trend was the decrease in Bare land and an increase in Urban Area and Steppe, indicating a shift towards anthropogenic land use. The classification and transitions are detailed in the confusion matrix (Table 5) and visualized changes (Figures 4 and 5). The detailed weighting values of explanatory variables and transitions between LULC classes are provided in Table 6 and Table 7, with the driving forces and their significance presented in Table 8.

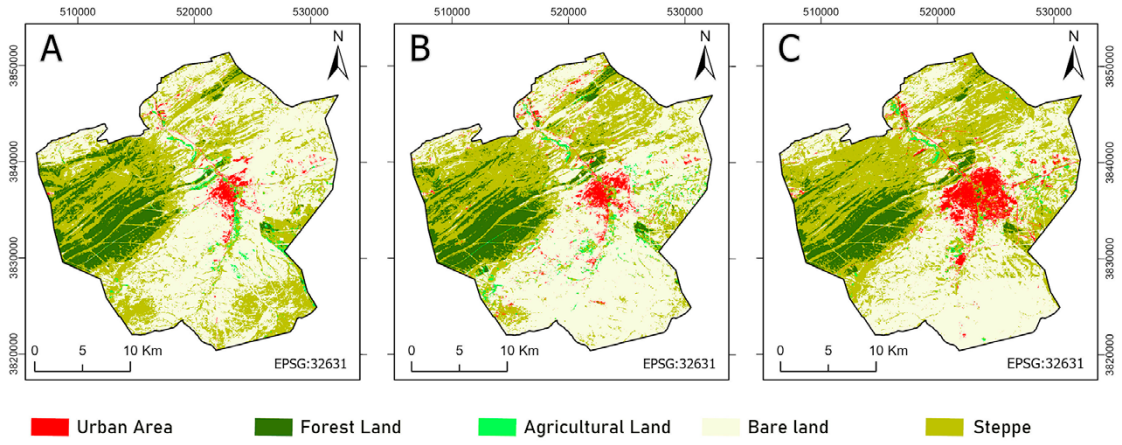

Figure 3. SVM classification results in GEE of (A) 1990, (B) 2005 and (C) 2020.

Table 4. Proportion of LULC units in 1990, 2005 and 2020

LULC unit	1990		2005		2020	
	Area (Ha)	Area (%)	Area (Ha)	Area (%)	Area (Ha)	Area (%)
Urban Area	924.09	1.75	1405.12	2.66	2742.30	5.20
Forest Land	6174.25	11.70	6128.76	11.61	5344.06	10.12
Agricultural Land	768.25	1.46	1051.47	1.99	547.05	1.04
Bare land	27944.39	52.94	28632.48	54.24	24976.58	47.32
Steppe	16974.66	32.16	15567.96	29,49	19175.79	36.33
Total	52785.64	100.00	52785.79	100.00	52785.79	100.00

Table 5. Confusion matrix of the LULC classification in 1990, 2005 and 2020

LULC 1990					
	Urban Area	Forest Land	Agricultural Land	Bare Land	Steppe
Urban Area	17	0	0	0	0
Forest Land	0	31	0	0	3
Agricultural Land	0	0	14	0	0
Bare land	0	0	1	32	3
Steppe	0	1	0	3	16
LULC 2005					
	Urban Area	Forest Land	Agricultural Land	Bare Land	Steppe
Urban Area	21	0	0	0	0
Forest Land	0	28	0	0	1
Agricultural Land	0	0	23	0	1
Bare land	1	0	2	26	1
Steppe	0	0	0	1	15
LULC 2020					
	Urban Area	Forest Land	Agricultural Land	Bare Land	Steppe
Urban Area	22	0	0	0	0
Forest Land	0	25	0	0	4
Agricultural Land	0	0	13	0	0
Bare land	0	0	0	27	0
Steppe	0	0	0	2	23

Table 6. Markov transitional probability matrix of land use types in Djelfa city based on (1990 to 2005), (2005 to 2020)

		LULC 1990				
		Urban Area	Forest Land	Agricultural Land	Bare Land	Steppe
LULC 2005	Urban Area	0.68	0.00	0.01	0.24	0.07
	Forest Land	0.00	0.84	0.00	0.00	0.16
	Agricultural Land	0.02	0.10	0.30	0.27	0.31
	Bare Land	0.02	0.00	0.02	0.84	0.12
	Steppe	0.01	0.05	0.02	0.28	0.64
		LULC 2005				
		Urban Area	Forest Land	Agricultural Land	Bare Land	Steppe
LULC 2020	Urban Area	0.71	0.01	0.01	0.13	0.14
	Forest Land	0.00	0.81	0.00	0.00	0.18
	Agricultural Land	0.05	0.05	0.16	0.21	0.53
	Bare Land	0.05	0.00	0.01	0.78	0.16
	Steppe	0.01	0.02	0.01	0.14	0.82

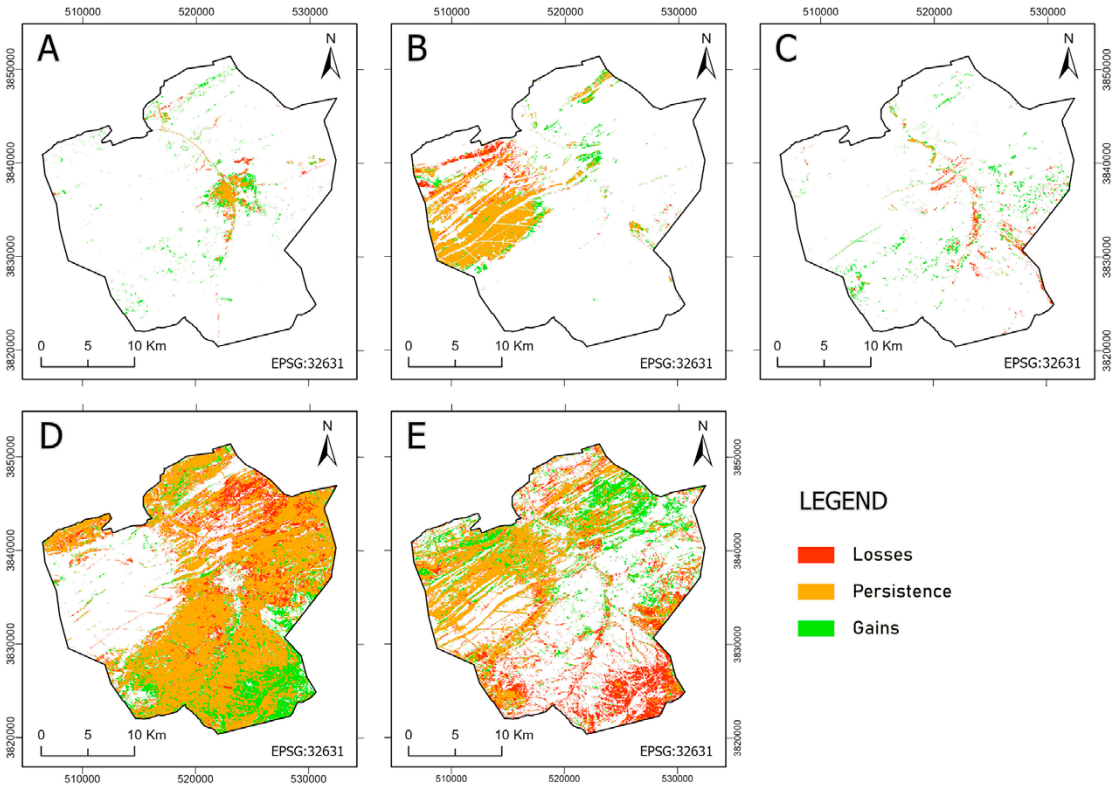

Figure 4. Gains and losses in various LULC between 1990 and 2005: (A) Urban Area, (B) Forest Land, (C) Agricultural Land, (D) Bare land, and (E) Steppe

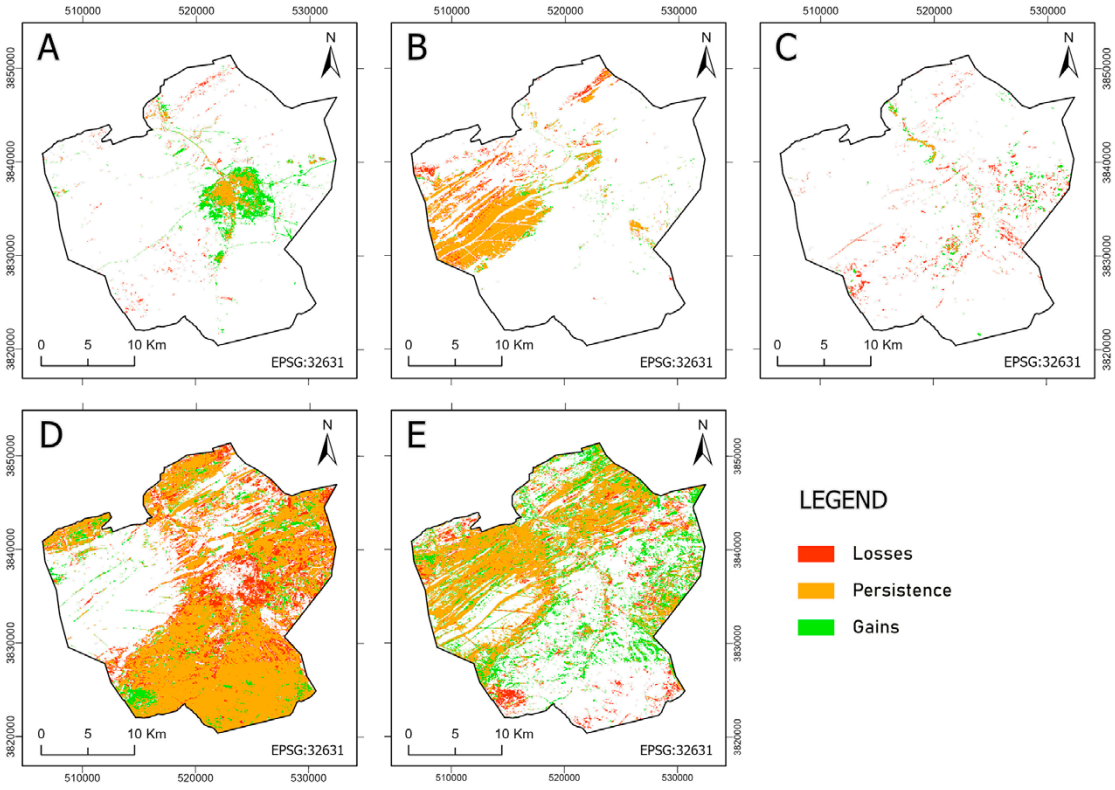

Figure 5. Gains and losses in various LULC between 2005 and 2020: (A) Urban Area, (B) Forest Land, (C) Agricultural Land, (D) Bare land, and (E) Steppe

Table 7. Driving forces with Cramer's V

Driving force	Cramer's V
Topographic map index	0.44
Distance from roads	0.49
Distance from the built up land	0.41
Distance to stream	0.27
Slope gradients	0.39
Elevation	0.62

Table 8. MLP model variable value and accuracy rate

Variables	Results
Hidden layer nodes	17
Start learning rate	0.01
End learning rate	0.001
Momentum factor	0.5
RMS	0.01
Iteration	10000
Training RMS	1
Testing RMS	1
Accuracy rate (%)	83.96
Skill measure	0.6791

Modeling LULC Transformation

The MLP method was employed for modeling the transformation potential for each LULC class. To facilitate this, an input dataset for the MultiLayer Perceptron, including spatial variables like elevation, distance from roads, and topographic index, was compiled and is illustrated in Figure 6. This groundwork led to the identification of nine significant transformations, which were then modeled and visualized in Figures 7 and 8. The process involved using the spatial variables mentioned earlier, leading to the generation of transition probability maps. These transitions underscore the region's dynamic land use, with a particular focus on the expansion of urban areas and the transformation of natural land cover types.

Model Validation

The validation process assessed the model's predictive accuracy using the Kappa coefficient (Table 9), comparing forecasted data with actual classified maps (Figure 9). The high Kappa value obtained signifies a robust fit and reliability of the model's predictions, suggesting the model's efficacy in forecasting future land cover dynamics. The kappa index values of the simulated LULC map for 2020, demonstrating the effectiveness of our model predictions, are presented in Table 10. This validation confirms the models' applicability for future LULC projections and the robustness of their predictions (Pontius, 2000).

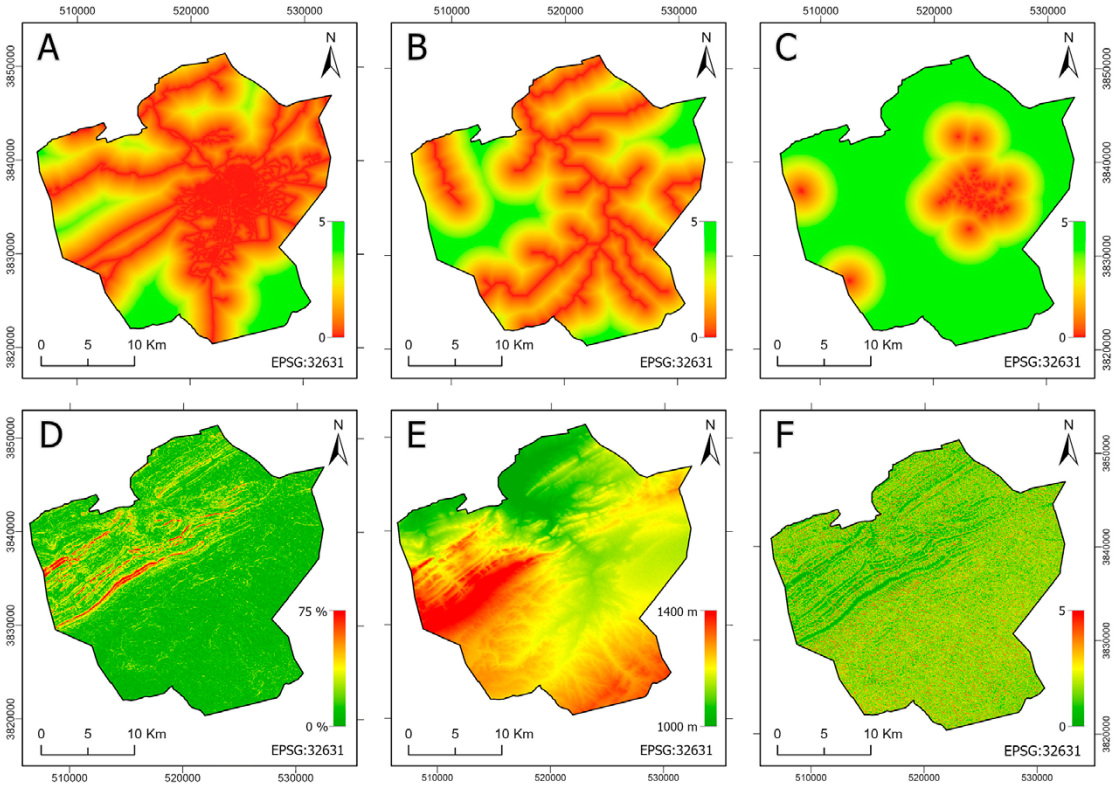

Figure 6. Input dataset for MultiLayer Perceptron: (A) Distance Road, (B) Distance stream hydro, (C) Distance urban, (D) Slope, (E) Elevation (DEM), and (F) Topographic map index

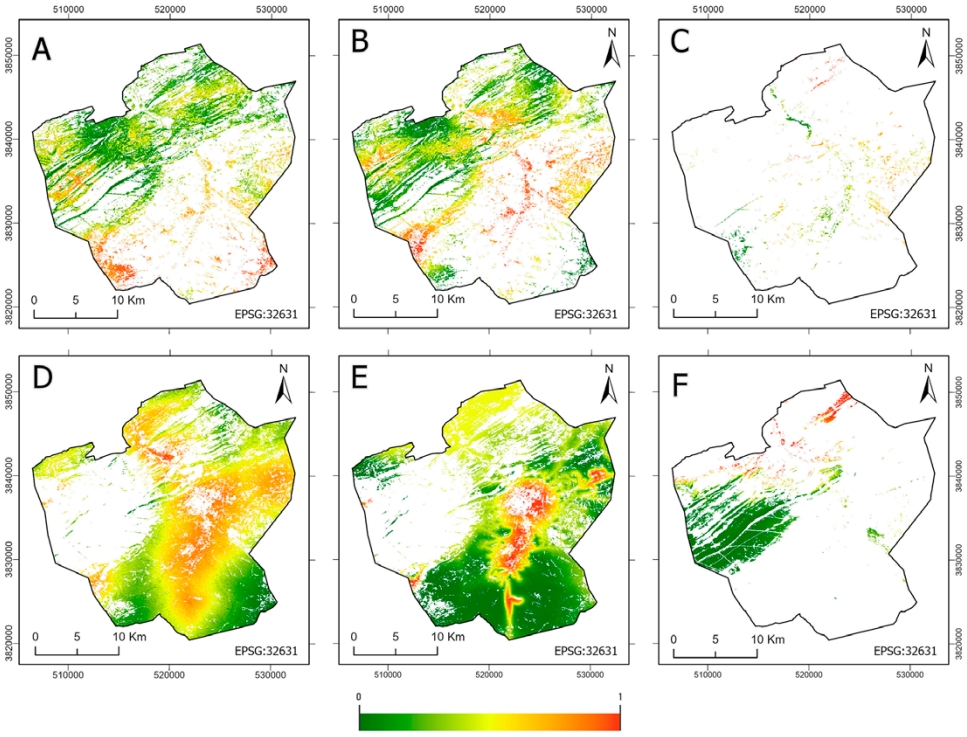

Figure 7. Major transformation. during 1990 to 2005; (A) from steppe to Bare land, (B) from steppe to Agricultural Land, (C) from Agricultural Land to Forest Land, (D) from Bare land to Agricultural Land, (E) from Bare land to Urban Area and (F) from Forest Land to steppe

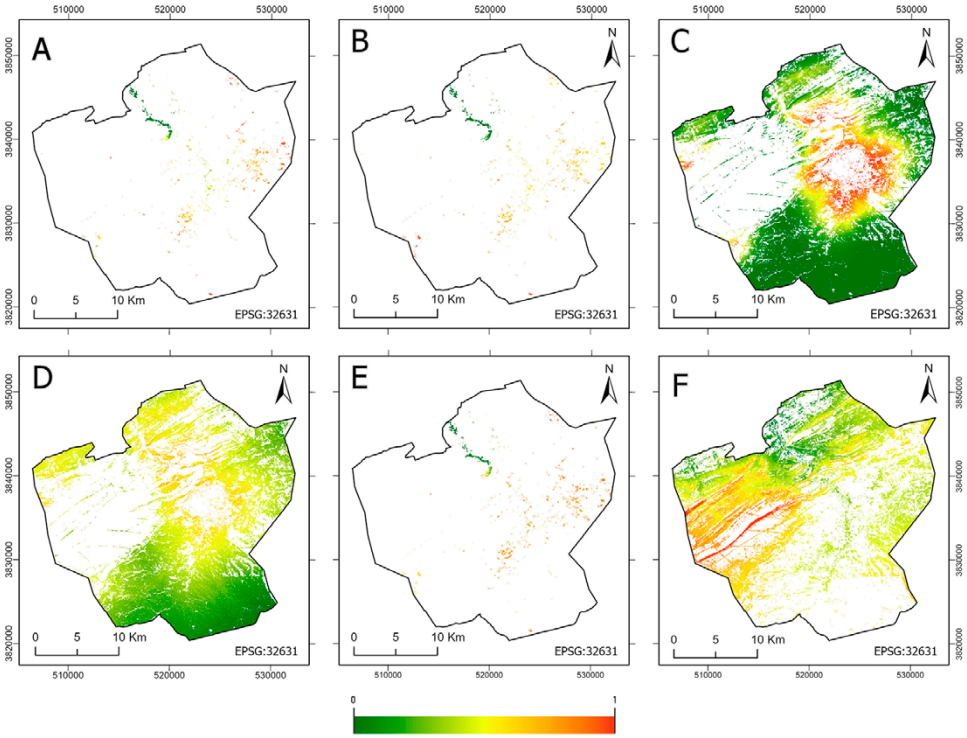

Figure 8. Major transformation. during 2005 to 2020; (A) from Agricultural Land to steppe, (B) from Agricultural Land to Forest Land, (C) from Bare land to Urban Area, (D) from Bare land to steppe, (E) from Agricultural Land to Urban Area and (F) from Forest Land to steppe

Table 9. LULC change prediction validation based on the actual and projected 2020 LULC

LULC Types	Projected 2020		Actual 2020	
	Area (Ha)	Area (%)	Area (Ha)	Area (%)
Urban Area	2742,30	5,20	2607,71	4,94
Agricultural Land	5344,06	10,12	5568,87	10,55
Forest Land	547,05	1,04	580,47	1,10
Steppe	24976,58	47,32	24862,69	47,10
Bare Land	19175,79	36,33	19166,05	36,31
Total	52785,79	100,00	52785,79	100,00

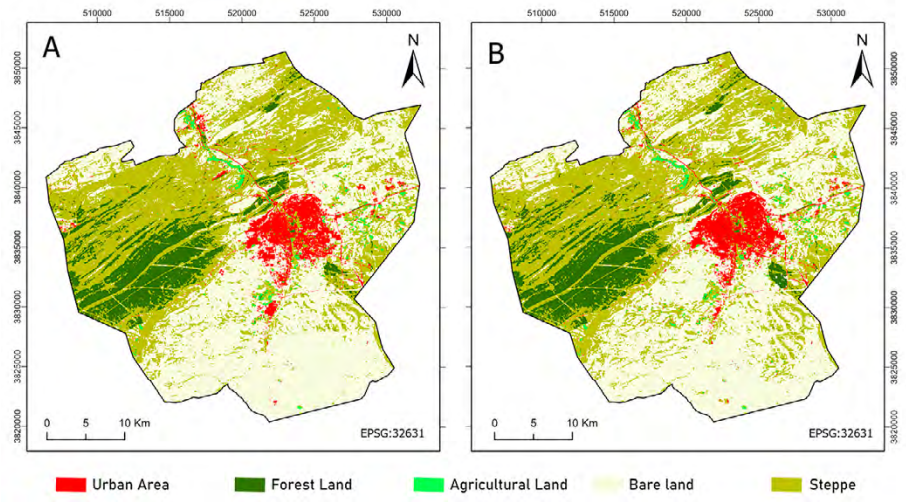

Figure 9. Observed and predicted LULC maps: (A) 2020 LULC observed, (B) 2020 LULC predicted

Table 10. The k index values of the simulated LULC map of 2020

Index	Value
Kno	0.9155
Klocation	0.8999
KlocationStrata	0.8999
Kstandard	0.8930

Future LULC Prediction

Future predictions using the MC model and LCM were validated and projected for 2035. Noteworthy transformations were categorized based on historical trends, with a particular increase in forested areas. The future LULC map for 2035, derived from the model, is presented in Figure 10, with a projected increase in Steppe and Urban Area, reflecting ongoing land rehabilitation efforts and urban expansion. The LULC coverage of classified and simulated images, which provides a comparative view of actual versus predicted land cover scenarios, is detailed in Table 11.

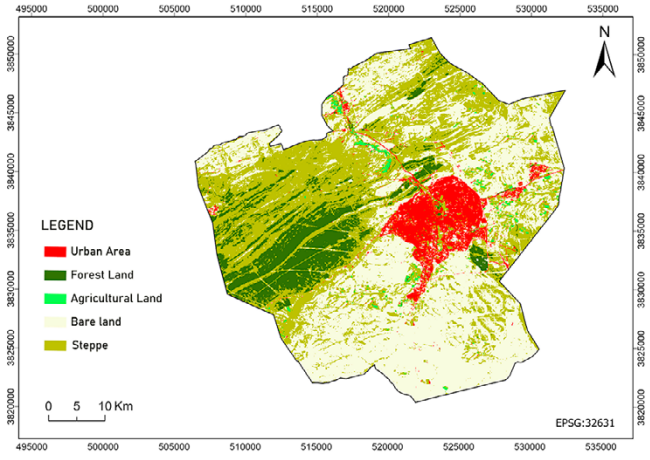

Figure 10. Predicted LULC map for 2035

Table 11. LULC coverage of classified and simulated images

LULC units	1990		2005		2020		2035	
	Area (Ha)	Area (%)	Area (Ha)	Area (%)	Area (Ha)	Area (%)	Area (Ha)	Area (%)
Urban Area	924.09	1.75	1405.12	2.66	2742.30	5.20	3588.93	6.80
Forest Land	6174.25	11.70	6128.76	11.61	5344.06	10.12	5576.99	10.57
Agricultural Land	768.25	1.46	1051.47	1.99	547.05	1.04	547.42	1.04
Bare Land	27944.39	52.94	28632.48	54.24	24976.58	47.32	24061.95	45.58
Steppe	16974.66	32.16	15567.96	29.49	19175.79	36.33	19010.48	36.01
Total	52785.64	100.00	52785.79	100.00	52785.79	100.00	52785.79	100.00

Discussion

In our study of multitemporal LULC mapping using SVM classification of Landsat imagery and auxiliary data within the GEE platform, we achieved high classification accuracy, underscoring the SVM method's robustness (Li et al., 2017). However, certain disparities in urban patterns between 1990 and 2005 were observed, notably in some urban areas undergoing significant changes. These variations may be attributed to challenges in acquiring high-quality images in dense cloud cover areas and phenological changes between seasons (Gong et al., 2016). Additionally, while employing images from December 2015 for our analysis, we postulated minimal land-cover change from our last ground truth sampling in May 2015, a factor that might have influenced our results.

The classification system occasionally diverged from global definitions, possibly leading to the misclassification of orchards and dense mixed crops as forests, particularly relevant in our ecological assessments (Gong et al., 2013). Recognizing such discrepancies is vital as they could contribute to the observed alterations in urban and other land cover categories. Despite these challenges, the overall accuracy rates of over 82.0% and corroborative visual observations of the maps emphasize SVM's significant utility and efficacy as a tool for LULC classification.

We reaffirm the strength and high accuracy of SVM classification in producing precise and consistent LULC maps and recognize the need for ongoing research. Future studies should explore the nuanced challenges and limitations encountered, particularly in urban area classification. Addressing these challenges will enhance the reliability and applicability of LULC maps, contributing to a more comprehensive understanding and management of land use and cover changes (Li et al., 2017). This continued effort is invaluable in advancing our understanding and appreciation of the dynamic and complex nature of land use classification.

Understanding LULC transitions is crucial for effective ecological and environmental management and gaining insights into future land use changes. Djelfa city, often referred to as the gateway to the Sahara or the capital of the steppes, provides a unique context for studying these transitions. Its landscape is marked by the Sennalba forest to the west, expansive steppe lands in the north, urban expansion to the east, and potential urban hubs in the south. Our study focused on analyzing LULC dynamics in Djelfa city over the past three decades and predicting future changes up to 2035. We employed various methodologies, including remote sensing, Geographic Information Systems (GIS), and a Multi-Layer Perceptron Neural Network (MLPNN)-based MC model, to comprehensively examine these dynamics.

The results revealed that Djelfa County has experienced a notable increase in urban expansion, driven by population growth and rural-to-urban migration This trend was particularly pronounced from 1990 to 2005 when the urban area expanded by 0.91% (D.P.S.B, 2020). Between 1987 and 1998, the population of Djelfa increased from 83,162 to 158,644 inhabitants, representing an annual growth rate of 6.67%. This surge can be partially attributed to the security situation between 1992 and 2001, which led rural residents and those from neighboring communities to migrate towards the city of Djelfa. From 1998 to 2008, the population growth accelerated, with the number rising to 311,931 inhabitants, at a growth rate of 6.6%—significantly higher than the national average. This growth was due to improved social conditions as evidenced by increased birth rates and decreased mortality rates. Moreover, the National Office of Statistics reports a positive internal migratory balance of 7,676 individuals and a positive external migratory balance of 1,660 individuals for Djelfa during this decade (ONS, 2011). These statistics not only substantiate a population increase but also support the urban expansion observed, correlating with the demographic growth and migration patterns.

Bare land, which covered a significant portion of the study area in 1990, experienced changes due to soil degradation, overgrazing, and pressures on rangelands. These changes may have been influenced not only by local land

management practices but also by broader environmental changes, including climate change, which can exacerbate soil erosion and desertification processes (IPCC, 2019; UN-OHRLLS, 2015). Agricultural land increased modestly from 1990 to 2005, mainly due to the abandonment of agropastoral activities during economic and security crises.

The forested area exhibited a decline, primarily attributed to anthropogenic pressures like illicit logging and overgrazing, while steppe areas witnessed significant expansion, partly due to land rehabilitation and silvicultural reclamation initiatives. Over the last decade to fifteen years, substantial rehabilitation efforts have been undertaken by the High Commission for Steppe Development (HCDS) and the National Forest Research Institute (INRF) Djelfa station. However, it's worth noting that this expansion isn't solely due to rehabilitation activities; microclimatic factors within the study area have also played a role in fostering steppe regeneration (Dudley & Phillips, 2006; World Economic Forum, 2023). The observed changes in our study area align with broader regional trends noted in other research, which have documented similar shifts in land cover types due to a combination of human activities and environmental changes (Alvarez Martinez et al., 2011).

The LULC classification and change analysis results corroborate the conversion of bare land into larger urban areas and steppe regions, with minor changes observed in agricultural and forested lands. This rise in steppe areas can be attributed to the aforementioned anthropogenic pressures, alongside the mentioned rehabilitation and silvicultural reclamation initiatives. Further research is needed to disentangle the relative impacts of these factors and to understand their interaction with climate change (Hart & Mouton, 2005; Keohane & Victor, 2011; Senge, 2008)

The observed land cover changes in our study from 2005 to 2020, such as decreasing forest cover and expanding urban and steppe areas, occur within a broader context of ecological fragility characteristic of arid and semi-arid regions. These regions, accounting for about 40% of Earth's land surface and including parts of North Africa, are particularly vulnerable to environmental changes (White & Nackoney, 2003; Yan et al., 2019). The trends noted in our study area are reflective of the challenges and dynamics experienced in these ecologically sensitive regions and align with documented patterns in similar contexts (Hishe et al., 2021). We acknowledge the importance of considering these broader ecological and geographical characteristics in our analysis and will further explore how these general trends manifest specifically in Algeria or Northwest Africa.

The projected LULC map for 2035 forecasts a further increase in urban areas, underscoring urbanization's continued influence on land use dynamics. This projection integrates a multi-index approach that improves the differentiation between urban build-up and bare soils, significantly enhancing classification accuracy, particularly in semi-arid regions like Djelfa. Notably, our model respects natural and man-made constraints, avoiding urban expansion into impractical areas such as the protected forest of Senelba, which aligns with the current concentric and compact urban form of Djelfa and similar cities within the Algerian steppe. Additionally, incorporating scenarios such as ecological protection, as suggested by (Xu et al., 2019), indicates a restrained urban spread compared to historical trends, which further confirms our projections' alignment with sustainable development practices. The precision of these projections could be improved with more detailed demographic data, yet the incorporation of various spectral indices and the consideration of geographical constraints assure the general reliability of our results. Future expansions are modeled to occur in viable areas, avoiding slopes or other inaccessible regions, thus reflecting a realistic trajectory of urban growth.

Our study highlights the dynamic nature of LULC changes in Djelfa city over the past 30 years and provides valuable insights for future land use planning. Sustainable urban development and effective land management strategies are essential to mitigate the environmental and social consequences of these changes. Monitoring and managing the pace and extent of urban expansion are critical to achieving sustainable development while preserving the environment. Furthermore, the integration of demographic data into future studies would provide a more holistic understanding of the drivers behind these changes, contributing to informed decision-making and effective management practices. Our use of ANN techniques has improved the reliability of our findings, reducing potential expert bias and inaccuracies in land cover analysis. However, it's important to note that the MLPNNMC approach may not cover all possible LULC transitions, and further research may be needed for applications involving a wider range of transitions, particularly in semi-natural areas.

Conclusion

In conclusion, this study utilized geospatial techniques and remote sensing data to analyze the temporal evolution of land use and land cover patterns in Djelfa city. By employing Landsat 5 and Landsat 8 imagery and employing advanced models, we projected land use changes up to 2035. Our validation process demonstrated the robustness of our approach, with an accuracy exceeding 83%, affirming the predictive capabilities of our composite model.

The integration of remote sensing, GIS, and land use change models proved to be a powerful tool for compre-

hensively mapping and monitoring land use transitions. Through SVM algorithms in GEE we generated accurate land use maps for pivotal years, highlighting the influence of auxiliary variables like elevation, roads, and settlement patterns on future land use changes.

Our analysis revealed a dominant trend towards urban expansion, resulting in a projected 6.80% increase in built-up areas by 2035. Additionally, our implementation of the Multi-Layer Perceptron MC model effectively estimated future land use dynamics, emphasizing the potential of remote sensing and GIS integration in land use analysis and prediction.

While our findings underscore the significance of our methodology for sustainable development and land management, we acknowledge the limitations related to the moderate resolution of Landsat imagery. This suggests room for improvement in image quality and prediction techniques for future research.

In summary, this research contributes to understanding and addressing the complex dynamics of land use in Djelfa city. By advocating for more comprehensive datasets, including climate, political, and urban development factors, we can enhance the accuracy of our predictive models. Replicating this methodology in other urban contexts will further enrich our insights into land use changes, guiding informed decisions for sustainable development while mitigating the environmental impacts of urban growth.

Acknowledgements

We extend our gratitude to the anonymous reviewers whose insightful feedback and constructive critiques significantly enhanced the quality of this manuscript. Our sincere appreciation also goes to the United States Geological Survey (USGS) for granting free access to the Landsat images utilized in this study.

Funding: *The research described in this study was not supported by any external funding sources.*

Conflicts of Interest: *The authors of this study have stated that there are no competing interests present.*

Disclosure: *The authors have no relevant financial or non-financial disclosures to report.*

Data Availability: *The datasets utilized and/or assessed in this study can be obtained by contacting the corresponding author upon reasonable request.*

Ethical approval: *All authors named in the manuscript have provided their consent for authorship, thoroughly reviewed and approved the manuscript, and granted permission for its submission and subsequent publication. The order of authorship was agreed upon by all listed authors before the manuscript was submitted.*

Ethical standards: *The manuscript has not been previously published, in part or in full, in any journal. It adheres to the ethical standards of this journal.*

References

Abijith, D., & Saravanan, S. (2022). Assessment of land use and land cover change detection and prediction using remote sensing and CA Markov in the northern coastal districts of Tamil Nadu, India. *Environmental Science and Pollution Research*, 29(57), 86055–86067. https://doi.org/10.1007/s11356-021-15782-6

Alqadhi, S., Mallick, J., Balha, A., Bindajam, A., Singh, C. K., & Hoa, P. V. (2021). Spatial and decadal prediction of land use/land cover using multi-layer perceptron-neural network (MLP-NN) algorithm for a semi-arid region of Asir, Saudi Arabia. *Earth Science Informatics*, 14(3), 1547–1562. https://doi.org/10.1007/s12145-021-00633-2

Alvarez Martinez, J. M., Suarez-Seoane, S., & De Luis Calabuig, E. (2011). Modelling the risk of land cover change from environmental and socio-economic drivers in heterogeneous and changing landscapes: The role of uncertainty. *Landscape and Urban Planning*, 101(2), 108–119. https://doi.org/10.1016/j.landurbplan.2011.01.009

Anand, J., Gosain, A. K., & Khosa, R. (2018). Prediction of land use changes based on Land Change Modeler and attribution of changes in the water balance of Ganga basin to land use change using the SWAT model. *Science of the Total Environment*, 644, 503–519. https://doi.org/10.1016/j.scitotenv.2018.07.017

Azari, M., Tayyebi, A., Helbich, M., & Reveshty, M. A. (2016). Integrating cellular automata, artificial neural network, and fuzzy set theory to simulate threatened orchards: Application to Maragheh, Iran. *GIScience and Remote Sensing*, 53(2), 183–205. https://doi.org/10.1080/15481603.2015.1137111

Barnieh, B. A., Jia, L., Menenti, M., Zhou, J., & Zeng, Y. (2020). Mapping land use land cover transitions at different spatiotemporal scales in West Africa. *Sustainability*, 12(20), 1–52. https://doi.org/10.3390/su12208565

Behera, M. D., Borate, S. N., Panda, S. N., Behera, P. R., & Roy, P. S. (2012). Modelling and analyzing the watershed dynamics using Cellular Automata (CA)-Mark-

ov model - A geo-information based approach. *Journal of Earth System Science*, 121(4), 1011–1024. https://doi.org/10.1007/s12040-012-0207-5

Beven, K. J., Kirkby, M. J., Schofield, N., & Tagg, A. F. (1984). Testing a Physically-Based Flood Forecasting Model (Topmodel) for Three U. K. Catchments. *Journal of Hydrology*, 69(1–4), 119–143.

Brown, D. G., Walker, R., Manson, S., & Seto, K. (2004). Modeling Land Use and Land Cover Change BT. In G. Gutman, A. C. Janetos, C. O. Justice, E. F. Moran, J. F. Mustard, R. R. Rindfuss, D. Skole, B. L. Turner, & M. A. Cochrane (Eds.), *Land Change Science: Observing, Monitoring and Understanding Trajectories of Change on the Earth's Surface* (pp. 395–409). Netherlands: Springer. https://doi.org/10.1007/978-1-4020-2562-4_23

Bullock, E. L., Healey, S. P., Yang, Z., Oduor, P., Gorelick, N., Omondi, S., Ouko, E., & Cohen, W. B. (2021). Three decades of land cover change in East Africa. *Land*, 10(2), 1–15. https://doi.org/10.3390/land10020150

Bununu, Y. A. (2017). Integration of Markov chain analysis and similarity-weighted instance-based machine learning algorithm (SimWeight) to simulate urban expansion. *International Journal of Urban Sciences*, 21(2), 217–237. https://doi.org/10.1080/12265934.2017.1284607

Camacho Olmedo, M. T., Pontius, R. G., Paegelow, M., & Mas, J. F. (2015). Comparison of simulation models in terms of quantity and allocation of land change. *Environmental Modelling and Software*, 69, 214–221. https://doi.org/10.1016/j.envsoft.2015.03.003

Carneiro, E., Lopes, W., & Espindola, G. (2021). Urban land mapping based on remote sensing time series in the google earth engine platform: A case study of the teresina-timon conurbation area in Brazil. *Remote Sensing*, 13(7). https://doi.org/10.3390/rs13071338

Chaudhuri, G., & Clarke, K. C. (2014). Temporal Accuracy in Urban Growth Forecasting: A Study Using the SLEUTH Model. *Transactions in GIS*, 18(2), 302–320. https://doi.org/10.1111/tgis.12047

Chen, H., & Pontius, R. G. (2010). Diagnostic tools to evaluate a spatial land change projection along a gradient of an explanatory variable. *Landscape Ecology*, 25(9), 1319–1331. https://doi.org/10.1007/s10980-010-9519-5

Congalton, R. G. (1991). A review of assessing the accuracy of classifications of remotely sensed data. *Remote Sensing of Environment*, 37(1), 35–46. https://doi.org/10.1016/0034-4257(91)90048-B

D.P.S.B. (2020). *Monograph of the wilaya of Djelfa*. Djelfa: Department of Budget Programming and Monitoring (3–11 pp).

Dong, J., Xiao, X., Menarguez, M. A., Zhang, G., Qin, Y., Thau, D., Biradar, C., & Moore, B. (2016). Mapping paddy rice planting area in northeastern Asia with Landsat 8 images, phenology-based algorithm and Google Earth Engine. *Remote Sensing of Environment*, 185, 142–154. https://doi.org/10.1016/j.rse.2016.02.016

Dudley, N., & Phillips, A. (2006). Forests and protected areas: guidance on the use of the IUCN protected area management categories. In Forests and protected areas : guidance on the use of the IUCN protected area management categories (Issue 12). https://doi.org/10.2305/iucn.ch.2006.pag.12.en

Dwivedi, R. S., Sreenivas, K., & Ramana, K. V. (2005). Land-use/land-cover change analysis in part of Ethiopia using Landsat Thematic Mapper data. *International Journal of Remote Sensing*, 26(7), 1285–1287. https://doi.org/10.1080/01431160512331337763

Eastman, J. R. (2015). *TerrSet Geospatial Monitoring and Modeling Software*. Clark University. https://clarklabs.org/terrset/

Eastman, J. R. (2020). *TerrSet Geospatial Monitoring and Modeling Software*. Clark University. https://clarklabs.org/terrset/

Ermida, S. L., Soares, P., Mantas, V., Göttsche, F. M., & Trigo, I. F. (2020). Google earth engine open-source code for land surface temperature estimation from the landsat series. *Remote Sensing*, 12(9), 1–21. https://doi.org/10.3390/RS12091471

Fadli, A. H., Kosugo, A., Ichii, K., & Ramli, R. (2019). Satellite-based monitoring of forest cover change in indonesia using google earth engine from 2000 to 2016. *Journal of Physics: Conference Series*, 1317(1), 012046. https://doi.org/10.1088/1742-6596/1317/1/012046

Fan, F., Weng, Q., & Wang, Y. (2007a). Land use and land cover change in Guangzhou, China, from 1998 to 2003, based on Landsat TM /ETM+ imagery. *Sensors*, 7(7), 1323–1342. https://doi.org/10.3390/s7071323

Fan, J. P. H., Wong, T. J., & Zhang, T. (2007b). Politically connected CEOs, corporate governance, and Post-IPO performance of China's newly partially privatized firms. *Journal of Financial Economics*, 84(2), 330–357. https://doi.org/10.1016/j.jfineco.2006.03.008

Feng, D., Zhao, Y., Yu, L., Li, C., Wang, J., Clinton, N., Bai, Y., Belward, A., Zhu, Z., & Gong, P. (2016). Circa 2014 African land-cover maps compatible with FROM-GLC and GLC2000 classification schemes based on multi-seasonal Landsat data. *International Journal of Remote Sensing*, 37(19), 4648–4664. https://doi.org/10.1080/01431161.2016.1218090

Feng, Y., Lei, Z., Tong, X., Gao, C., Chen, S., Wang, J., & Wang, S. (2020). Spatially-explicit modeling and intensity analysis of China's land use change 2000–2050. *Journal of Environmental Management*, 263, 110407. https://doi.org/10.1016/j.jenvman.2020.110407

Findell, K. L., Berg, A., Gentine, P., Krasting, J. P., Lintner, B. R., Malyshev, S., Santanello, J. A., & Shevliakova, E. (2017). The impact of anthropogenic land use and land cover change on regional climate extremes. *Na-*

ture Communications, 8(1), 1–9. https://doi.org/10.1038/s41467-017-01038-w

Gashaw, T., Tulu, T., Argaw, M., & Worqlul, A. W. (2018). Modeling the hydrological impacts of land use/land cover changes in the Andassa watershed, Blue Nile Basin, Ethiopia. *Science of the Total Environment*, 619–620, 1394–1408. https://doi.org/10.1016/j.scitotenv.2017.11.191

Gong, P., Wang, J., Yu, L., Zhao, Y., Zhao, Y., Liang, L., Niu, Z., Huang, X., Fu, H., Liu, S., Li, C., Li, X., Fu, W., Liu, C., Xu, Y., Wang, X., Cheng, Q., Hu, L., Yao, W., Zhang, H., Zhu, P., Zhao, Z, Zhang, H., Zheng, Y., Ji, L., Zhang, Y., Chen, H., Yan, A., Guo, J., Yu, L., Wang, L., Liu, X., Shi, T., Zhu, M., Chen, Y., Yang, G., Tang, P., Xu, B., Giri, C., Clinton, N., Zhu, Z., & Chen, J. (2013). Finer resolution observation and monitoring of global land cover: First mapping results with Landsat TM and ETM+ data. *International Journal of Remote Sensing*, 34(7), 2607–2654. https://doi.org/10.1080/01431161.2012.748992

Gong, P., Yu, L., Li, C., Wang, J., Liang, L., Li, X., Ji, L., Bai, Y., Cheng, Y., & Zhu, Z. (2016). A new research paradigm for global land cover mapping. *Annals of GIS*, 22(2), 87–102. https://doi.org/10.1080/19475683.2016.1164247

Gorelick, N., Hancher, M., Dixon, M., Ilyushchenko, S., Thau, D., & Moore, R. (2017). Google Earth Engine: Planetary-scale geospatial analysis for everyone. *Remote Sensing of Environment*, 202(2016), 18–27. https://doi.org/10.1016/j.rse.2017.06.031

Green, K., Kempka, D., & Lackey, L. (1994). Using remote sensing to detect and monitor land-cover and land-use change. *Photogrammetric Engineering and Remote Sensing*, 60, 331–337.

Hackman, K. O., Gong, P., & Wang, J. (2017). New land-cover maps of Ghana for 2015 using landsat 8 and three popular classifiers for biodiversity assessment. *International Journal of Remote Sensing*, 38(14), 4008–4021. https://doi.org/10.1080/01431161.2017.1312619

Hackman, K. O., Li, X., Asenso-Gyambibi, D., Asamoah, E. A., & Nelson, I. D. (2020). Analysis of geo-spatiotemporal data using machine learning algorithms and reliability enhancement for urbanization decision support. *International Journal of Digital Earth*, 13(12), 1717–1732. https://doi.org/10.1080/17538947.2020.1805036

Halmy, M. W. A., Gessler, P. E., Hicke, J. A., & Salem, B. B. (2015). Land use/land cover change detection and prediction in the north-western coastal desert of Egypt using Markov-CA. *Applied Geography*, 63, 101–112. https://doi.org/10.1016/j.apgeog.2015.06.015

Hart, T., & Mouton, J. (2005). Indigenous knowledge and its relevance for agriculture: a case study in Uganda. *Indilinga African Journal of Indigenous Knowledge Systems*, 4(1), 249–263.

Hasan, S., Shi, W., Zhu, X., Abbas, S., & Khan, H. U. A. (2020). Future simulation of land use changes in rapidly urbanizing South China based on land change modeler and remote sensing data. *Sustainability*, 12(11), 4–6. https://doi.org/10.3390/su12114350

Hishe, H., Giday, K., Van Orshoven, J., Muys, B., Taheri, F., Azadi, H., Feng, L., Zamani, O., Mirzaei, M., & Witlox, F. (2021). Analysis of Land Use Land Cover Dynamics and Driving Factors in Desa'a Forest in Northern Ethiopia. *Land Use Policy*, 101, 105039. https://doi.org/10.1016/j.landusepol.2020.105039

Homer, C., Dewitz, J., Jin, S., Xian, G., Costello, C., Danielson, P., Gass, L., Funk, M., Wickham, J., & Stehman, S. (2020). Conterminous United States land cover change patterns 2001–2016 from the 2016 national land cover database. *ISPRS Journal of Photogrammetry and Remote Sensing*, 162, 184–199.

Hu, Y., Dong, Y., & Batunacun. (2018). An automatic approach for land-change detection and land updates based on integrated NDVI timing analysis and the CVAPS method with GEE support. ISPRS *Journal of Photogrammetry and Remote Sensing*, 146, 347–359. https://doi.org/10.1016/j.isprsjprs.2018.10.008

IPCC. (2019). Climate Change and Land: an IPCC special report. Climate Change and Land: An IPCC Special Report on Climate Change, Desertification, Land Degradation, Sustainable Land Management, Food Security, and Greenhouse Gas Fluxes in Terrestrial Ecosystems, 1–864. https://www.ipcc.ch/srccl/

Islam, K., Rahman, M. F., & Jashimuddin, M. (2018). Modeling land use change using Cellular Automata and Artificial Neural Network: The case of Chunati Wildlife Sanctuary, Bangladesh. *Ecological Indicators*, 88, 439–453. https://doi.org/10.1016/j.ecolind.2018.01.047

Karul, C., & Soyupak, S. (2003). A Comparison between Neural Network Based and Multiple Regression Models for Chlorophyll-a Estimation BT. In F. Recknagel (Ed.), *Ecological Informatics: Understanding Ecology by Biologically-Inspired Computation* (pp. 249–263). Berlin Heidelberg: Springer. https://doi.org/10.1007/978-3-662-05150-4_13

Keohane, R. O., & Victor, D. G. (2011). The regime complex for climate change. *Perspectives on Politics*, 9(1), 7–23.

Kim, Y., & Newman, G. (2020). Advancing scenario planning through integrating urban growth prediction with future flood risk models. *Computers, Environment and Urban Systems*, 82, 101498. https://doi.org/10.1016/j.compenvurbsys.2020.101498

Kolb, M., Mas, J. F., & Galicia, L. (2013). Evaluating drivers of land-use change and transition potential models in a complex landscape in Southern Mexico. *International Journal of Geographical Information Science*, 27(9), 1804–1827. https://doi.org/10.1080/13658816.2013.770517

Lambin, E. F. (1997). Modelling and monitoring land-cover change processes in tropical regions. *Progress in Physical Geography*, 21(3), 375–393. https://doi.org/10.1177/030913339702100303

Larbi, I., Forkuor, G., Hountondji, F. C. C., Agyare, W. A., & Mama, D. (2019). Predictive Land Use Change under Business-As-Usual and Afforestation Scenarios in the Vea Catchment, West Africa. *International Journal of Advanced Remote Sensing and GIS*, 8(1), 3011–3029. https://doi.org/10.23953/cloud.ijarsg.416

Li, C., Gong, P., Wang, J., Zhu, Z., Biging, G. S., Yuan, C., Hu, T., Zhang, H., Wang, Q., Li, X., Liu, X., Xu, Y., Guo, J., Liu, C., Hackman, K. O., Zhang, M., Cheng, Y., Yu, L., Yang, J., Huang, H., & Clinton, N. (2017). The first all-season sample set for mapping global land cover with Landsat-8 data. *Science Bulletin*, 62(7), 508–515. https://doi.org/10.1016/j.scib.2017.03.011

Li, J., Knapp, D. E., Lyons, M., Roelfsema, C., Phinn, S., Schill, S. R., & Asner, G. P. (2021). Automated global shallowwater bathymetry mapping using google earth engine. *Remote Sensing*, 13(8). https://doi.org/10.3390/rs13081469

Liu, C., Li, W., Zhu, G., Zhou, H., Yan, H., & Xue, P. (2020). Land use/land cover changes and their driving factors in the northeastern tibetan plateau based on geographical detectors and google earth engine: A case study in gannan prefecture. *Remote Sensing*, 12(19), 1–18. https://doi.org/10.3390/RS12193139

Liu, G., Jin, Q., Li, J., Li, L., He, C., Huang, Y., & Yao, Y. (2017). Policy factors impact analysis based on remote sensing data and the CLUE-S model in the Lijiang River Basin, China. *Catena*, 158, 286–297. https://doi.org/10.1016/j.catena.2017.07.003

López, E., Bocco, G., Mendoza, M., & Duhau, E. (2001). Predicting land-cover and land-use change in the urban fringe. *Landscape and Urban Planning*, 55(4), 271–285. https://doi.org/10.1016/s0169-2046(01)00160-8

Mantero, P., Moser, G., & Serpico, S. B. (2004). Partially supervised classification of remote sensing images using SVM-based probability density estimation. *IEEE Transactions on geoscience and remote sensing*, 43(3), 559-570. https://doi.org/10.1109/WARSD.2003.1295212

Mao, L., & Li, M. (2021). Integrating Sentinel Active and Passive Data to Map Land Cover in a National Park from GEE Platform. *Geomatics and Information Science of Wuhan University*, 48(5), 756-764.

Mas, J. F., Kolb, M., Paegelow, M., Camacho Olmedo, M. T., & Houet, T. (2014). Inductive pattern-based land use/cover change models: A comparison of four software packages. *Environmental Modelling and Software*, 51, 94–111. https://doi.org/10.1016/j.envsoft.2013.09.010

Mather., A. S. (1986). *Land use*. Longman.

Midekisa, A., Holl, F., Savory, D. J., Andrade-Pacheco, R., Gething, P. W., Bennett, A., & Sturrock, H. J. W. (2017). Mapping land cover change over continental Africa using Landsat and Google Earth Engine cloud computing. *PLoS ONE*, 12(9), 1–15. https://doi.org/10.1371/journal.pone.0184926

Mirici, M. E., Berberoglu, S., Akin, A., & Satir, O. (2018). Land use/cover change modelling in a mediterranean rural landscape using multi-layer perceptron and markov chain (MLP-MC). *Applied Ecology and Environmental Research*, 16(1), 467–486. https://doi.org/10.15666/aeer/1601_467486

Mishra, V. N., & Rai, P. K. (2016). A remote sensing aided multi-layer perceptron-Markov chain analysis for land use and land cover change prediction in Patna district (Bihar), India. *Arabian Journal of Geosciences*, 9(4). https://doi.org/10.1007/s12517-015-2138-3

Mishra, V. N., Rai, P. K., Prasad, R., Punia, M., & Nistor, M. M. (2018). Prediction of spatio-temporal land use/land cover dynamics in rapidly developing Varanasi district of Uttar Pradesh, India, using geospatial approach: a comparison of hybrid models. *Applied Geomatics*, 10(3), 257–276. https://doi.org/10.1007/s12518-018-0223-5

Mozumder, C., Tripathi, N. K., & Losiri, C. (2016). Comparing three transition potential models: A case study of built-up transitions in North-East India. *Computers, Environment and Urban Systems*, 59, 38–49. https://doi.org/10.1016/j.compenvurbsys.2016.04.009

Mugiraneza, T., Nascetti, A., & Ban, Y. (2020). Continuous monitoring of urban land cover change trajectories with landsat time series and landtrendr-google earth engine cloud computing. *Remote Sensing*, 12(18). https://doi.org/10.3390/RS12182883

Noma, A., Korting, T. S., & Fonseca, L. M. G. (2013). Uma Comparação entre Classificadores usando Regiões e Perfis EVI para Agricultura. *Anais XVI Simpósio Brasileiro de Sensoriamento Remoto, São José dos Campos: Instituto Nacional de Pesquisas Espaciais*, 2250-2257. http://urlib.net/dpi.inpe.br/marte2/2013/05.28.23.34

Nowak, D. J., & Greenfield, E. J. (2020). The increase of impervious cover and decrease of tree cover within urban areas globally (2012–2017). *Urban Forestry and Urban Greening*, 49. https://doi.org/10.1016/j.ufug.2020.126638

Oliveira, J. P. (2017). Detecção de áreas desmatadas na porção sul do estado do Amazonas, utilizando técnicas de extração de características e redes neurais artificiais. Master thesis. Manaus: Universidade Federal do Amazonas, Faculdade de Technologia.

ONS. (2011). L'armature urbaine RGPH 2008 - Collections Statistiques n° 163/2011 [The urban framework RGPH 2008 - Statistics Collections n° 163/2011]. 220. https://www.ons.dz/IMG/pdf/armature_urbaine_2008.pdf

Pérez-Vega, A., Mas, J. F., & Ligmann-Zielinska, A. (2012). Comparing two approaches to land use/cover change modeling and their implications for the assessment of biodiversity loss in a deciduous tropical forest. *Environmental Modelling and Software*, 29(1), 11–23. https://doi.org/10.1016/j.envsoft.2011.09.011

Pontius, R. G. (2000). Quantification error versus location error in comparison of categorical maps. *Photogrammetric Engineering and Remote Sensing*, 67(5), 540-540.

Pontius, R. G., Boersma, W., Castella, J. C., Clarke, K., Nijs, T., Dietzel, C., Duan, Z., Fotsing, E., Goldstein, N., Kok, K., Koomen, E., Lippitt, C. D., McConnell, W., Mohd Sood, A., Pijanowski, B., Pithadia, S., Sweeney, S., Trung, T. N., Veldkamp, A. T., & Verburg, P. H. (2008). Comparing the input, output, and validation maps for several models of land change. *Annals of Regional Science*, 42(1), 11–37. https://doi.org/10.1007/s00168-007-0138-2

Prasomsup, W., Piyatadsananon, P., Aunphoklang, W., & Boonrang, A. (2020). Extraction technic for built-up area classification in Landsat 8 imagery. *International Journal of Environmental Science and Development*, 11(1), 15–20. https://doi.org/10.18178/ijesd.2020.11.1.1219

Rawat, J. S., & Kumar, M. (2015). Monitoring land use/cover change using remote sensing and GIS techniques: A case study of Hawalbagh block, district Almora, Uttarakhand, India. *Egyptian Journal of Remote Sensing and Space Science*, 18(1), 77–84. https://doi.org/10.1016/j.ejrs.2015.02.002

Roy, S., Pandit, S., Eva, E. A., Bagmar, M. S. H., Papia, M., Banik, L., Dube, T., Rahman, F., & Razi, M. A. (2020). Examining the nexus between land surface temperature and urban growth in Chattogram Metropolitan Area of Bangladesh using long term Landsat series data. *Urban Climate*, 32, 100593. https://doi.org/10.1016/j.uclim.2020.100593

Senge, P. (2008). The necessary revolution: How individuals and organisations are working together to create a sustainable world. *Management Today*, 24(10), 54–57.

Shaharum, N. S. N., Shafri, H. Z. M., Ghani, W. A. W. A. K., Samsatli, S., Al-Habshi, M. M. A., & Yusuf, B. (2020). Oil palm mapping over Peninsular Malaysia using Google Earth Engine and machine learning algorithms. *Remote Sensing Applications: Society and Environment*, 17, 100287. https://doi.org/10.1016/j.rsase.2020.100287

Shawul, A. A., & Chakma, S. (2019). Spatiotemporal detection of land use/land cover change in the large basin using integrated approaches of remote sensing and GIS in the Upper Awash basin, Ethiopia. *Environmental Earth Sciences*, 78(5), 1–13. https://doi.org/10.1007/s12665-019-8154-y

Singh, A. (1989). Review Articlel: Digital change detection techniques using remotely-sensed data. *International Journal of Remote Sensing*, 10(6), 989–1003. https://doi.org/10.1080/01431168908903939

Singh, S. K., Laari, P. B., Mustak, S. K., Srivastava, P. K., & Szabó, S. (2018). Modelling of land use land cover change using earth observation data-sets of Tons River Basin, Madhya Pradesh, India. *Geocarto International*, 33(11), 1202–1222.

Sinha, S., Sharma, L. K., & Nathawat, M. S. (2015). Improved Land-use/Land-cover classification of semi-arid deciduous forest landscape using thermal remote sensing. *Egyptian Journal of Remote Sensing and Space Science*, 18(2), 217–233. https://doi.org/10.1016/j.ejrs.2015.09.005

Siroosi, H., Heshmati, G., & Salmanmahiny, A. (2020). Can empirically based model results be fed into mathematical models? MCE for neural network and logistic regression in tourism landscape planning. *Environment, Development and Sustainability*, 22(4), 3701–3722. https://doi.org/10.1007/s10668-019-00363-y

Skole, D., & Tucker, C. (1993). Tropical deforestation and habitat fragmentation in the amazon: Satellite data from 1978 to 1988. *Science*, 260(5116), 1905–1910. https://doi.org/10.1126/science.260.5116.1905

UN-OHRLLS. (2015). The Impact of Climate Change, Desertification and Land Degradation on the Development Prospects of Landlocked Developing Countries. 1–59. http://unohrlls.org/custom-content/uploads/2015/11/Impact_Climate_Change_2015.pdf

Wagle, N., Acharya, T. D., Kolluru, V., Huang, H., & Lee, D. H. (2020). Multi-temporal land cover change mapping using google earth engine and ensemble learning methods. *Applied Sciences*, 10(22), 1–20. https://doi.org/10.3390/app10228083

Wahap, N. A., & Shafri, H. Z. M. (2020). Utilization of Google Earth Engine (GEE) for land cover monitoring over Klang Valley, Malaysia. *IOP Conference Series: Earth and Environmental Science*, 540(1). https://doi.org/10.1088/1755-1315/540/1/012003

Wang, J., Wu, J., Wang, Z., Gao, F., & Xiong, Z. (2020). Understanding Urban Dynamics via Context-Aware Tensor Factorization with Neighboring Regularization. IEEE *Transactions on Knowledge and Data Engineering*, 32(11), 2269–2283. https://doi.org/10.1109/TKDE.2019.2915231

White, R. P., & Nackoney, J. (2003). *Drylands, people, and ecosystem goods and services*. World resources institute.

Winkler, K., Fuchs, R., Rounsevell, M., & Herold, M. (2021). Global land use changes are four times greater than previously estimated. *Nature Communications*, 12(1), 1–10. https://doi.org/10.1038/s41467-021-22702-2

World Economic Forum. (2023). The Global Risks Report 2023 (18.a). In The WEF. https://www.weforum.org/reports/global-risks-report-2023

Xiong, J., Thenkabail, P. S., Gumma, M. K., Teluguntla, P., Poehnelt, J., Congalton, R. G., Yadav, K., & Thau, D. (2017). Automated cropland mapping of continental Africa using Google Earth Engine cloud computing. *ISPRS Journal of Photogrammetry and Remote Sensing*, 126, 225–244. https://doi.org/10.1016/j.isprsjprs.2017.01.019

Xiong, Y., Xu, W., Lu, N., Huang, S., Wu, C., Wang, L., Dai, F., & Kou, W. (2021). Assessment of spatial–temporal changes of ecological environment quality based on RSEI and GEE: A case study in Erhai Lake Basin, Yun-

nan province, China. *Ecological Indicators*, 125, 107518. https://doi.org/10.1016/j.ecolind.2021.107518

Xu, C., McDowell, N. G., Fisher, R. A., Wei, L., Sevanto, S., Christoffersen, B. O., Weng, E., & Middleton, R. S. (2019). Increasing impacts of extreme droughts on vegetation productivity under climate change. *Nature Climate Change*, 9(12), 948–953. https://doi.org/10.1038/s41558-019-0630-6

Yan, Q., Le, P. V. V., Woo, D. K., Hou, T., Filley, T., & Kumar, P. (2019). Three-Dimensional Modeling of the Coevolution of Landscape and Soil Organic Carbon. *Water Resources Research*, 1218–1241. https://doi.org/10.1029/2018WR023634

Yu, L., Liang, L., Wang, J., Zhao, Y., Cheng, Q., Hu, L., Liu, S., Yu, L., Wang, X., Zhu, P., Li, X., Xu, Y., Li, C., Fu, W., Li, X., Li, W., Liu, C., Cong, N., Zhang, H., Fangdi, S., Xinfang, B., Xin, Q., Li, D., Yan, D., Zhu, Z., Goodchild, M. F. & Gong, P. (2014). Meta-discoveries from a synthesis of satellite-based land-cover mapping research. *International Journal of Remote Sensing*, 35(13), 4573–4588. https://doi.org/10.1080/01431161.2014.930206

Zadbagher, E., Becek, K., & Berberoglu, S. (2018). Modeling land use/land cover change using remote sensing and geographic information systems: case study of the Seyhan Basin, Turkey. *Environmental Monitoring and Assessment*, 190(8). https://doi.org/10.1007/s10661-018-6877-y

Zhao, G. X., Lin, G., & Warner, T. (2004). Using Thematic Mapper data for change detection and sustainable use of cultivated land: A case study in the Yellow River delta, China. *International Journal of Remote Sensing*, 25(13), 2509–2522. https://doi.org/10.1080/0143116031000161957 1

Zhao, Z., Meng, Y., Yue, A., Huang, Q., Kong, Y., Yuan, Y., Liu, X., Lin, L., & Zhang, M. (2016). Review of remotely sensed time series data for change detection. *Yaogan Xuebao/Journal of Remote Sensing*, 20(5), 1110–1125. https://doi.org/10.11834/jrs.20166170